NASA TECHNICAL NOTE

NASA TN D-3359

AEROBEE 150 PROPULSION FAILURE

by J. R. Busse and P. S. Bushnell, Jr.

Goddard Space Flight Center
Greenbelt, Md.

NATIONAL AERONAUTICS AND SPACE ADMINISTRATION • WASHINGTON, D. C. • FEBRUARY 1967

AEROBEE 150 PROPULSION FAILURE

By J. R. Busse and P. S. Bushnell, Jr.

Goddard Space Flight Center
Greenbelt, Md.

NATIONAL AERONAUTICS AND SPACE ADMINISTRATION

ABSTRACT

NASA vehicle 4.113 GA-GI, an Aerobee 150 launched from the White Sands Missile Range, New Mexico in April 1964, experienced a "hard" start (an explosive initial combustion generating high chamber pressures) which resulted in other anomalies, including a tail can explosion after 27 seconds of flight. The most probable cause of the hard start was an improper rupture sequence of the fuel and oxidizer diaphragms which could have resulted from an improper fuel bleed or manufacturing discrepancies. As a result of corrective measures, no hard starts occurred in eighteen later Aerobee flights in 1964.

CONTENTS

AEROBEE 150 PROPULSION FAILURE

by
J. R. Busse and P. S. Bushnell, Jr.
Goddard Space Flight Center

INTRODUCTION

NASA vehicle 4.113 GA-GI, an Aerobee 150 launched from the White Sands Missile Range, New Mexico on 21 April 1964, experienced a "hard" start (an explosive initial combustion generating high chamber pressures) which resulted in other anomalies including a tail can explosion after 27 seconds of flight. This report describes an investigation of this propulsion system failure, including an analysis of flight performance data and flight films, and corrective action taken to avoid a recurrence in future flights.

PREFLIGHT PREPARATION

Aerobee 150 rocket 4.113 GA-GI (sustainer NASA 97-3) was prepared for launching by Navy personnel at the U.S. Naval Ordnance Test Facility, White Sands with the assistance of Goddard Space Flight Center (GSFC) and Space General Corporation (SGC) personnel in accordance with detailed check sheets issued by SGC and approved by NASA/GSFC. The rocket was originally shipped from El Monte, California to the Churchill Research Range, Manitoba, Canada but was later sent to WSMR via Railway Express.

No major discrepancies were noted during the manufacture of sustainer 97-3 by SGC and no abnormal conditions were noted during rocket checkout; however, during the 100 psig gas leak test, a leak was observed at the fuel and oxidizer propellant tank fill ports. The fuel and oxidizer gas burst diaphragms were removed and inspected. Proper torquing of the gas orifice nuts upon re-installation eliminated the leak. The 15 psig leak checks were performed and checks were made for leaks through the propellant diaphragms at the thrust chamber nozzle. All "B"-nuts and fittings were set with Loctite sealant or safety-wired and then leak-checked. The pressure switch on the helium fill line was pressure tested and installed in the forward skirt.

The rocket was then transferred to the monorail laboratory for the horizontal payload test. According to normal procedure, horizontal payload checks were performed, the rocket was weighed, and the center of gravity was determined. The payload was removed, weighed, and the center of gravity was computed for use in determining payload instability during recovery.

Following mating of the sustainer with the booster, the rocket was transported to the launch tower and installed. The helium tank was subjected to 400 and 3,000 psig leak tests in the tower. Vertical payload checks were commenced following the attachment of the payload to the rocket. After a difficulty with the umbilical connector was corrected, the -5 hour payload check was performed.

1

Following a final inspection of the rocket, the NASA representatives left the tower to observe the propellant-servicing operation from the edge of the launch pad. No difficulties were experienced with the oxidizer pumping system but a problem with the fuel pump caused a slight delay in the fueling operation. The pumping problem was corrected by Navy personnel. Final tower inspection was performed following propellant servicing. The booster igniter was installed and the helium tank was pressurized to an indicated 3,450 psig.

LAUNCH AND FLIGHT PERFORMANCE

The firing of NASA 4.113 GA-GI was accompanied by a loud bang and the rocket emitted an unusual sound variously described as a whine, a scream, or a low-pitched whistle in leaving the tower. The flame and smoke did not appear normal, the booster being partially obscured by a dense cloud of smoke which was reddish brown (Figure 1), in contrast to the usual orange sustainer flame and almost gray-white exhaust trail from the booster propellant combustion of normal flights (Figure 2).
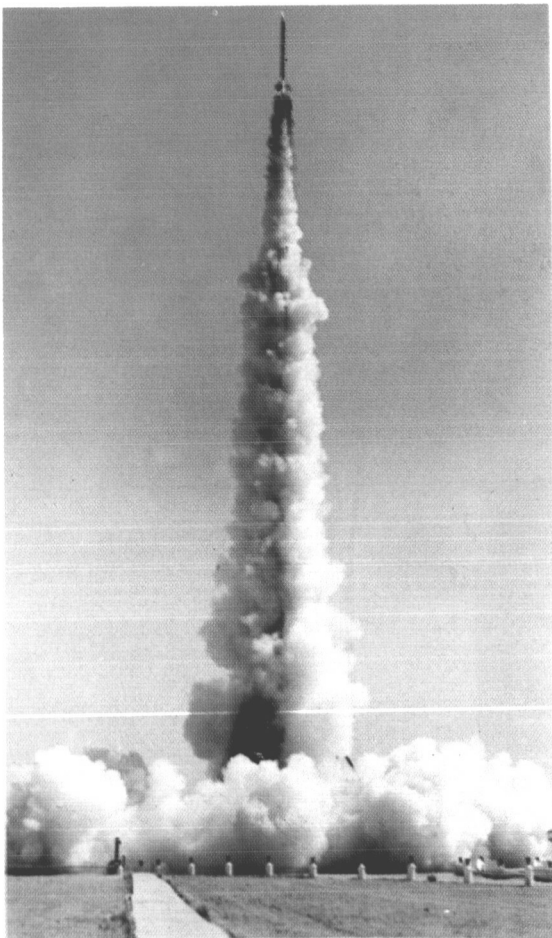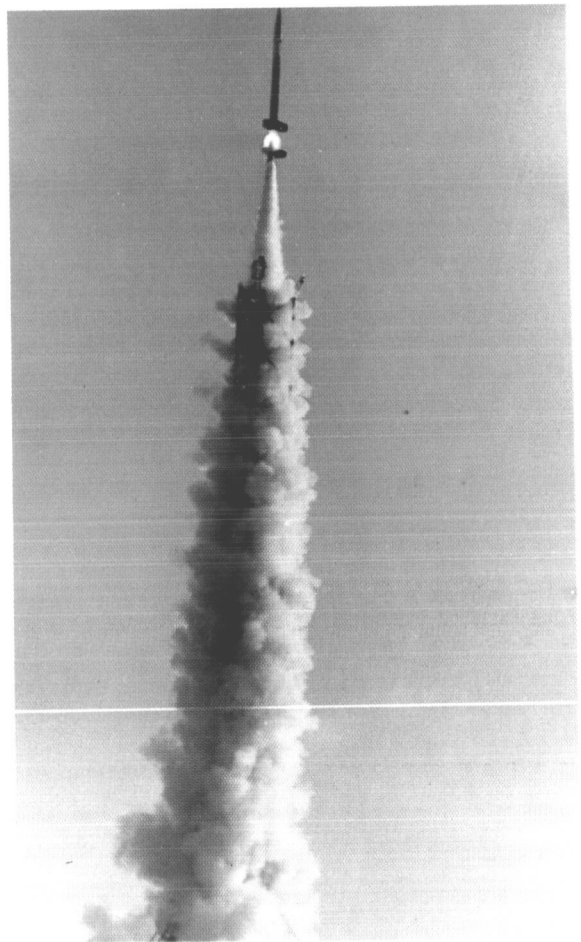

Figure 1—NASA 4.113 GA-GI launching from WSMR.

Figure 2—A normal Aerobee 150 leaving the tower at WSMR (NASA 4.67 NP).

Figure 3—Aft bulkhead of fuel tank and thrust
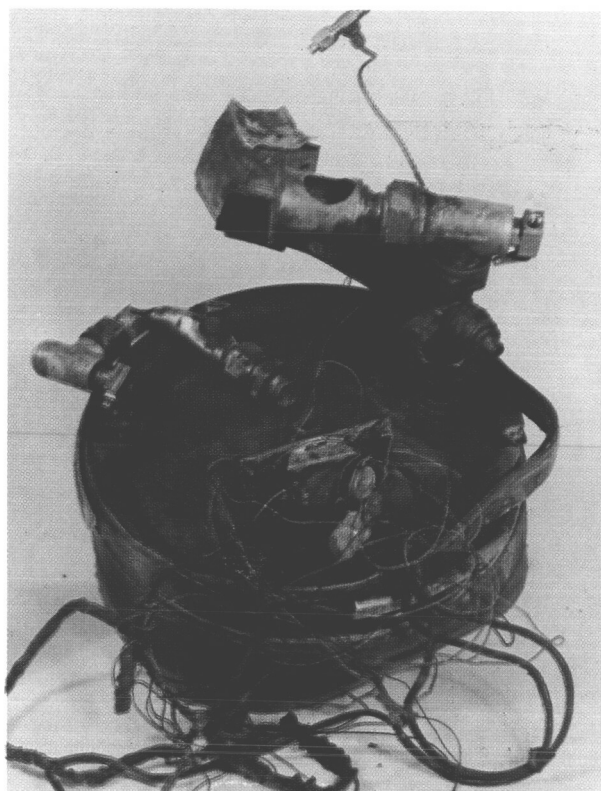structure of motor after removal from tankage.

Figure 4—Fuel tank bulkhead
separated from the tankage.

Observers outside the blockhouse saw a brilliant white flash approximately 27 seconds after launch, which was assumed to have resulted from an explosion of the tail section. The dense red-dish brown exhaust cloud characterizing the launch was viewed throughout the entire flight. Movies were taken of the rocket through apogee to impact approximately five miles from the launch tower. Due to the low altitude and brief duration of the flight, none of its experimental objectives was realized.

POSTFLIGHT INSPECTION

Postflight inspection of the rocket revealed that the tail can, sustainer fins and fuel coolant tap were missing. Also, the chamber pressure tap was broken. Only one of the fins with a portion of the tail can magnesium skin was found after a search of the entire area. However, there was no evidence of melting or burning on these parts of the recovered propulsion system plumbing. Some damage had been sustained by the rocket from the impact—the thrust structure was bent and the propellant tankage was dented.

Clearly visible in Figure 3, which shows the aft bulkhead of the fuel tank and the motor thrust structure, is an aniline residue on the outside of the thrust chamber. The fuel line is broken just

between the B-nut and the attachment to the fuel tank bulkhead. Subsequent metallurgical analysis of this fracture at GSFC substantiated the assumption of an impact fracture of this piece.

Figure 4 also illustrates this bulkhead covered with a burned aniline residue, except in the area in line with the chamber pressure connector. The chamber pressure connector and the control and instrumentation wiring were clean and showed no traces of heating. The plumbing was coated with the aniline residue, the heaviest coating appearing on the forward side of the components. There was little or no residue on the under side. Residue was also noted on the edges of the hole created by the missing fuel tap and the broken chamber pressure tap was heavily coated (a diagram of the propulsion system identifying the various parts discussed in the report is given in Figure 5).
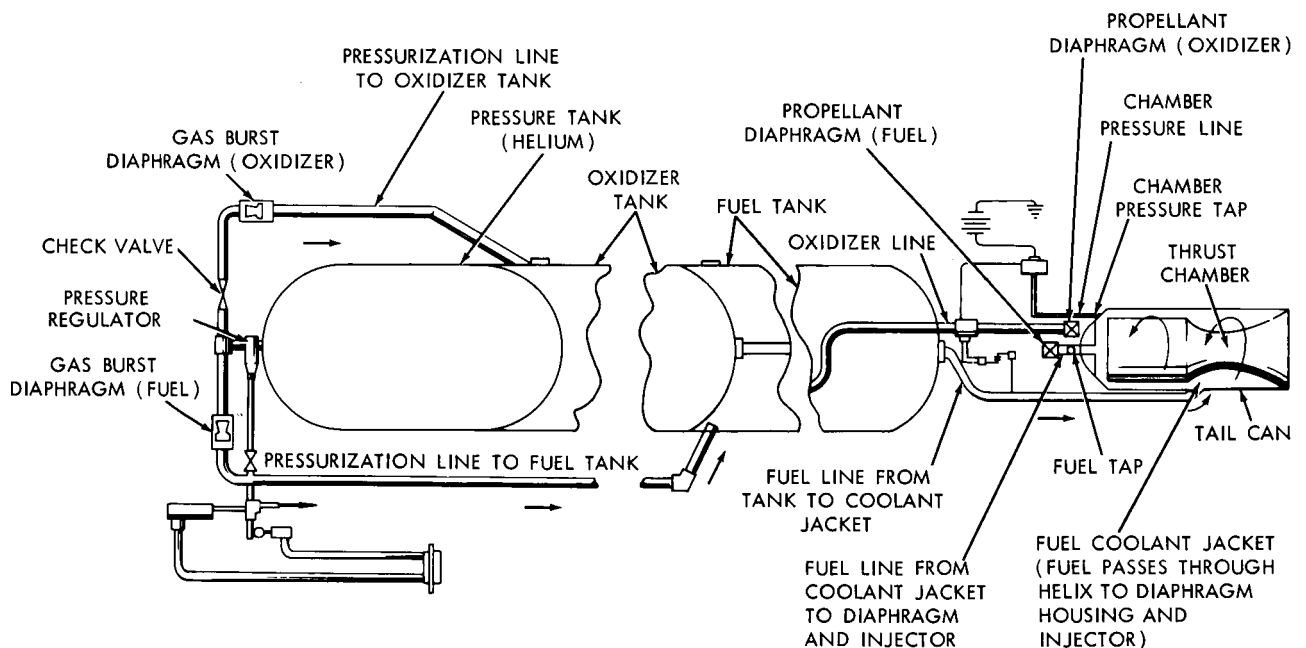
Figure 5—Diagram of Aerobee 150 propulsion system.

Figure 6a shows the rocket motor after removal. Figure 6b is a close-up view illustrating the missing tap on the propellant line from the coolant jacket to the fuel injector, and the broken chamber pressure tap covered with the residue. Metallurgical analysis at GSFC of the mode of fracture of the propellant line tap indicated that it failed by application of a force in the opposite direction to the force that would have been applied by impact, a fact which was instrumental in establishing the failure of the tap during the hard start and in explaining subsequent performance.

Figure 6a—Rocket motor after disassembly.
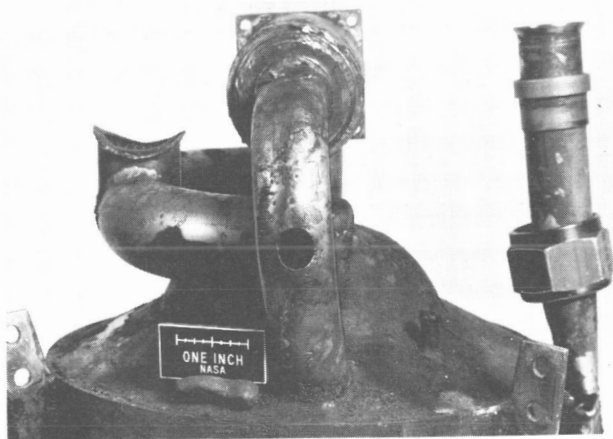
Figure 6b—Close-up view of damage sustained by rocket motor.
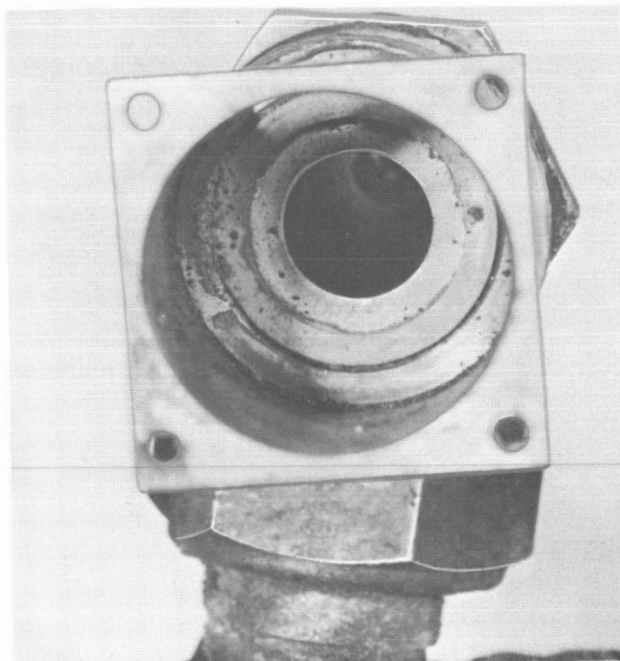
Figure 7—Mixture ratio orifice.

The mixture ratio orifice (Figure 7) was still in its proper place and of the proper size (0.78 in.). Also, if may be observed that the outer ring on the oxidizer burst diaphragm was still intact in its proper position. The fuel and oxidizer strainer cages (Figure 8) were inspected. A trapped "O"-ring that was dislodged from the fuel shutoff valve may be seen in a close-up view of the fuel strainer in Figure 9. The shutoff valves were in the open position.

The helium pressure regulator was removed and returned to the manufacturer for flow tests. The aft bulkhead was removed and returned to GSFC along with plumbing and motor parts. The motor and plumbing were disassembled, inspected, photographed, and submitted for metallurgical examination.

Figure 8—Fuel and oxidizer strainers.
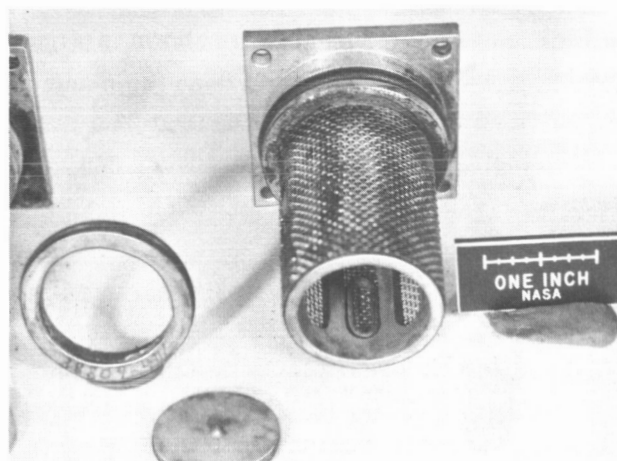
Figure 9—An "O"-ring wedged in the fuel strainer.

DATA REDUCTION

Chamber pressure, magnetometer, and acceleration telemetry data were received, reduced, and plotted. Both Contraves and radar metric data were used to provide trajectory data. Tracking and documentary films of the flight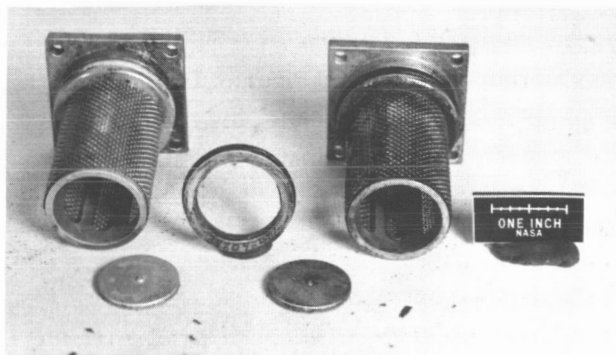, both 16 and 35 mm color and black-and-white, were carefully studied and compared with similar films for successful Aerobee 150 launchings.

Chamber Pressure

Telemetry data based on voltage ratios from preflight calibration curves (Figure 10) show that chamber pressure rose rapidly to 190 psia at 0.06 seconds after ignition and continued to build up erratically, reaching a maximum of 330 psia at 0.49 seconds (Figure 11). (Presumably the frequency response of the Giannini pressure transducer was inadequate to record the maximum pressure encountered during the hard start.) It then fell off drastically. The initial peak followed by the erratic buildup and sharp dropoff were significant factors indicating areas for investigation.
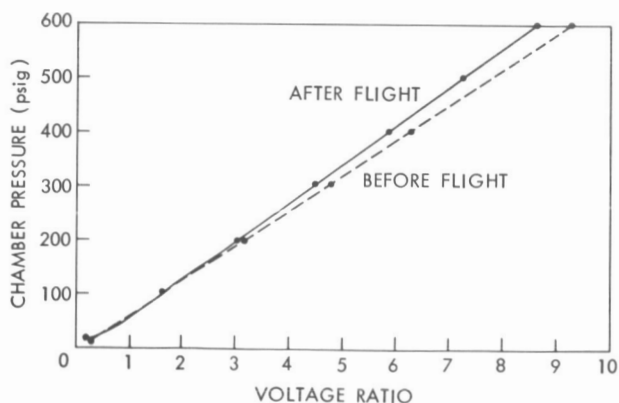
Figure 10—Comparison of preflight and postflight pressure transducer calibration.
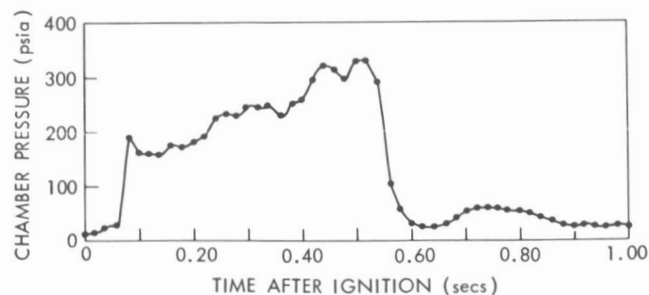
Figure 11—Chamber pressure during the first second of flight.

6

Chamber pressure data from 0.8 seconds to the loss of the signal at 27.5 seconds, based on a recalibration of the transducer, is shown in Figure 12. The postflight chamber pressure transducer calibrations were slightly higher than the manufacturer's plotted calibration (Figures 10 and 12). Chamber pressure began to increase at 23.5 seconds of flight and at 27.5 seconds, the point at which telemetry was lost, the transducer gage read 85 psi (which was subsequently presumed to be tail can pressure).
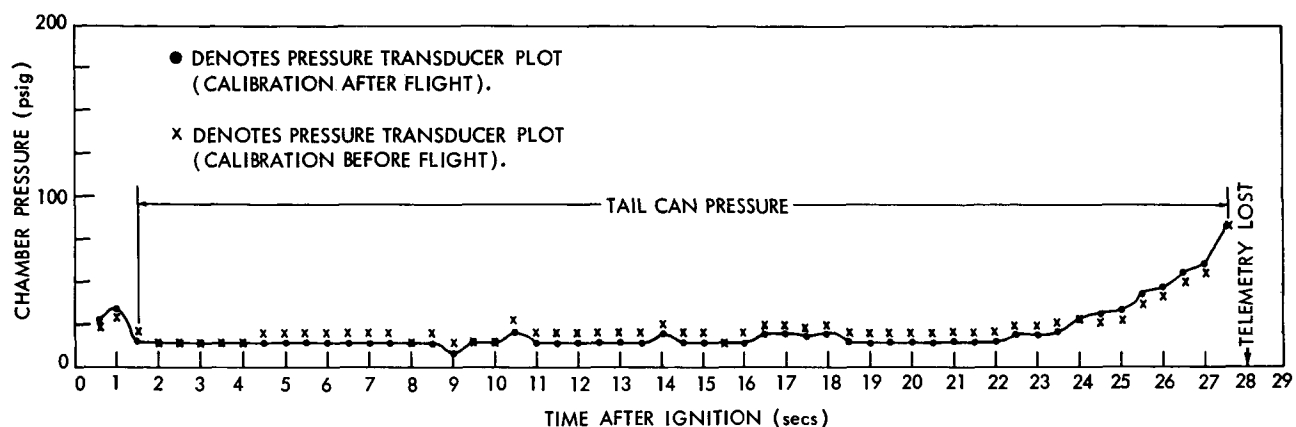
Figure 12—Pressure transducer readings.
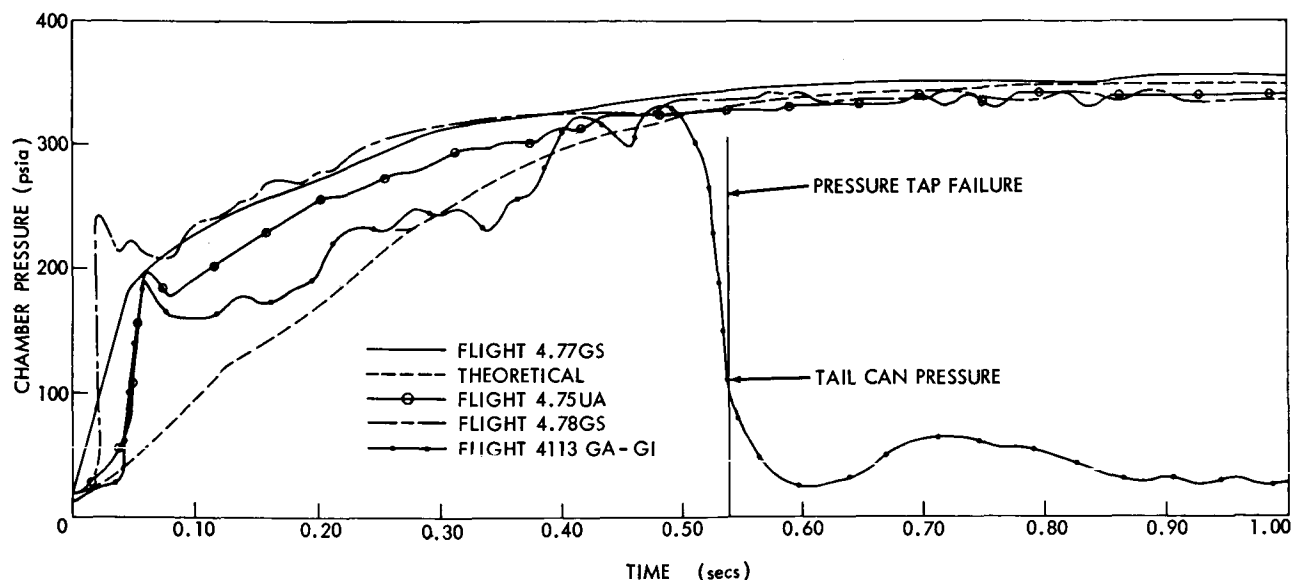
Figure 13—Comparative start transient chamber pressure data.

Figure 13 presents several normal chamber pressure transducer plots compared to the start transient trace for NASA 4.113 GA-GI. Also included is a theoretical chamber pressure curve. The erratic performance of NASA 4.113 GA-GI can readily be noted.

Acceleration

Acceleration curves were plotted from both telemetry (Figure 14) and Contraves data (Figure 15). The telemetry acceleration data are now considered to be of questionable value compared to the more reliable data produced from Contraves optical tracking, which was excellent throughout the flight.

According to both telemetry and Contraves data, acceleration reached 10 g during the first 2.5 seconds, dropping to 1 g after booster burnout (2.5 seconds). Both data sources were in agreement within 0.1 g from booster burnout until 9 seconds.

From telemetry, acceleration began to increase again at 9 seconds, reaching 1.6 g at 12 seconds. It increased again at 13 seconds reaching 3.5 g at 17 seconds. Between 17 and 19 seconds, it reached four major peaks, fluctuating between 3.5 to 4.5 g. No explanation has been deduced for this abnormal behavior, other than that it was possibly due to accelerometer resonance during flight caused by the erratic chamber operation, or rocket coning motion producing a centrifugal acceleration. Acceleration decreased gradually to 1.6 g between 19 and 24 seconds. At 25 seconds, another period of erratic acceleration was experienced until telemetry was lost at 27.5 seconds.

According to Contraves optical tracking data, acceleration did not drop below 1 g from 9.4 seconds until the loss of Contraves data at 26.5 seconds, and reached peaks of 1.75 g and 2.2 g at 25 seconds and 26.5 seconds, respectively. Generally, observed acceleration was a little low, although not
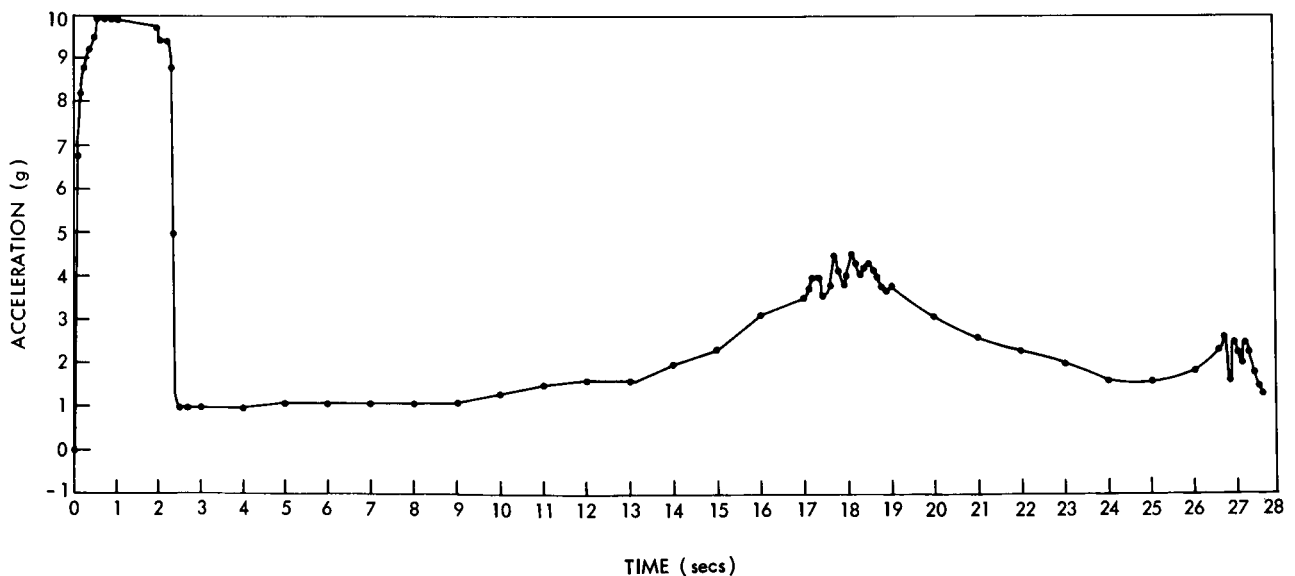
Figure 14—Telemetry acceleration data.
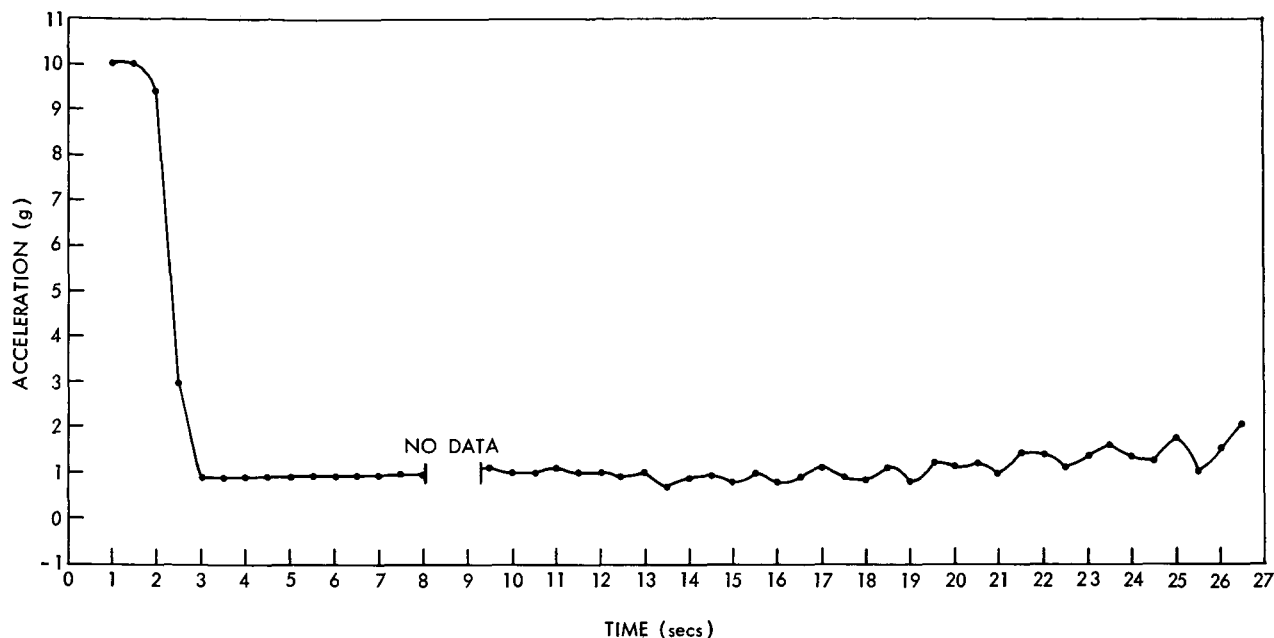
Figure 15—Contraves optical tracking acceleration data.

too abnormal. This performance could be obtained from a rocket operating under an extreme mix-ture ratio condition. (The normal 150 mixture ratio is 2.56 to 1, oxidizer to fuel.)

The acceleration data substantiate the failure of the pressure tap, as the observed acceleration could not have been obtained from chamber pressure as that recorded by the transducer.

Velocity

The velocity data received from reduced Contraves trajectory data indicated that the rocket was traveling at 735 fps at booster burnout (Figure 16). The velocity at 26.5 seconds, when track-ing was lost, was 1575 fps. A later integration of acceleration curves from Contraves and telemetry instrumentation data indicated velocities of 1644 and 2292 fps, respectively, the latter being less reliable data. Compared to the velocity expected of a normal Aerobee 150 flight, the observed velocities were low but the increase was steady.

Altitude

Figure 17 shows the altitude performance for the flight plotted from smoothed radar data. Figure 18 illustrates an expected performance trajectory for a rocket of similar payload weight and launch elevation. The sustainer should have burned out at 51.8 seconds at an altitude of 129,445 feet. Actually, all combustion was completed between 46 and 47 seconds, with a loss of effective propulsion at 27.4 seconds when the tail can was lost and the vehicle went into a violent tumbling and flat spinning motion. It was the tumbling (high drag) rocket motion which caused the vehicle to descend slowly. Whereas the altitude at 27.4 seconds should have been somewhere be-tween 40,000-50,000 feet, it was only 34,000 feet.
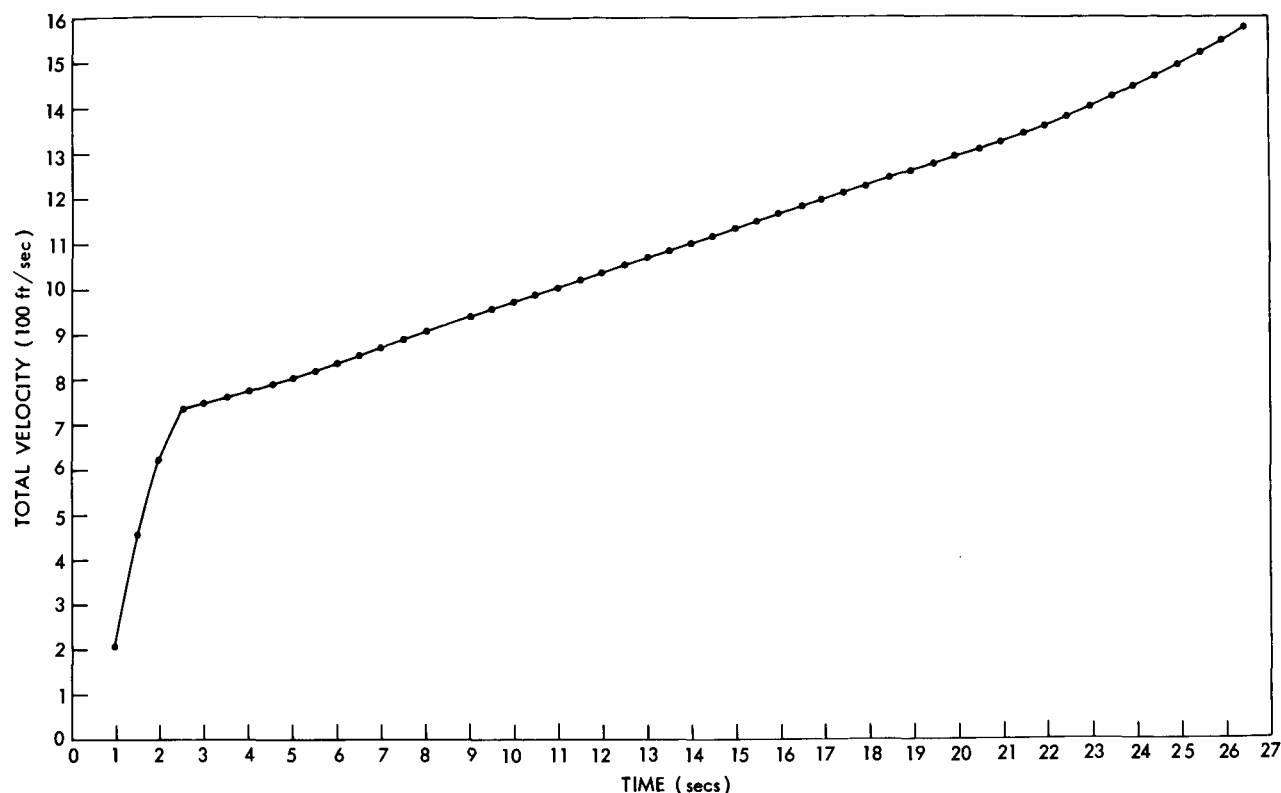
Figure 16—Contraves trajectory velocity data.

FILM COVERAGE

Photographic records taken during the flight of NASA 4.113 GA-GI were excellent. Film coverage included black-and-white motion pictures taken by two WSMR tracking stations, color motion pictures taken from two documentary cameras at the launch site, and a color photograph of the launch.

The color photograph of the launch, (Figure 1) clearly illustrates the unusual colored exhaust which lasted through the flight. Also, excellent black-and-white films taken the first seconds of launch provided detailed views of the vehicle going up the tower. The sequence in Figure 19, taken at the rate of 20 frames per second, indicates the hard start. Note the shape of the flame, and also the abnormally large flash, which was a result of high-pressure start conditions.

The sustainer ignited 0.2 to 0.3 seconds after booster ignition. The booster ignition was considered to be the first flame from which smoke could be recognized in the black-and-white tracking
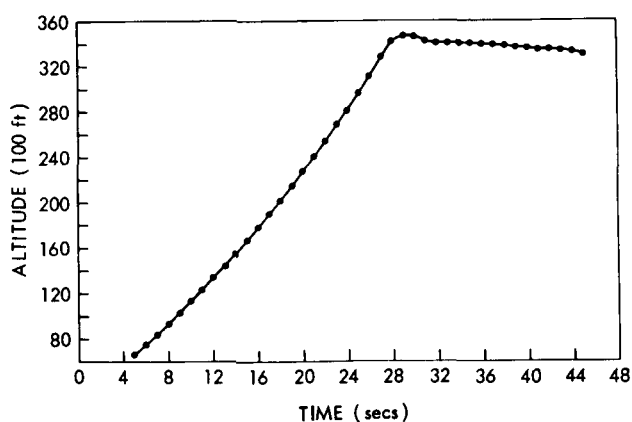
Figure 17—Altitude vs. time (smoothed radar).
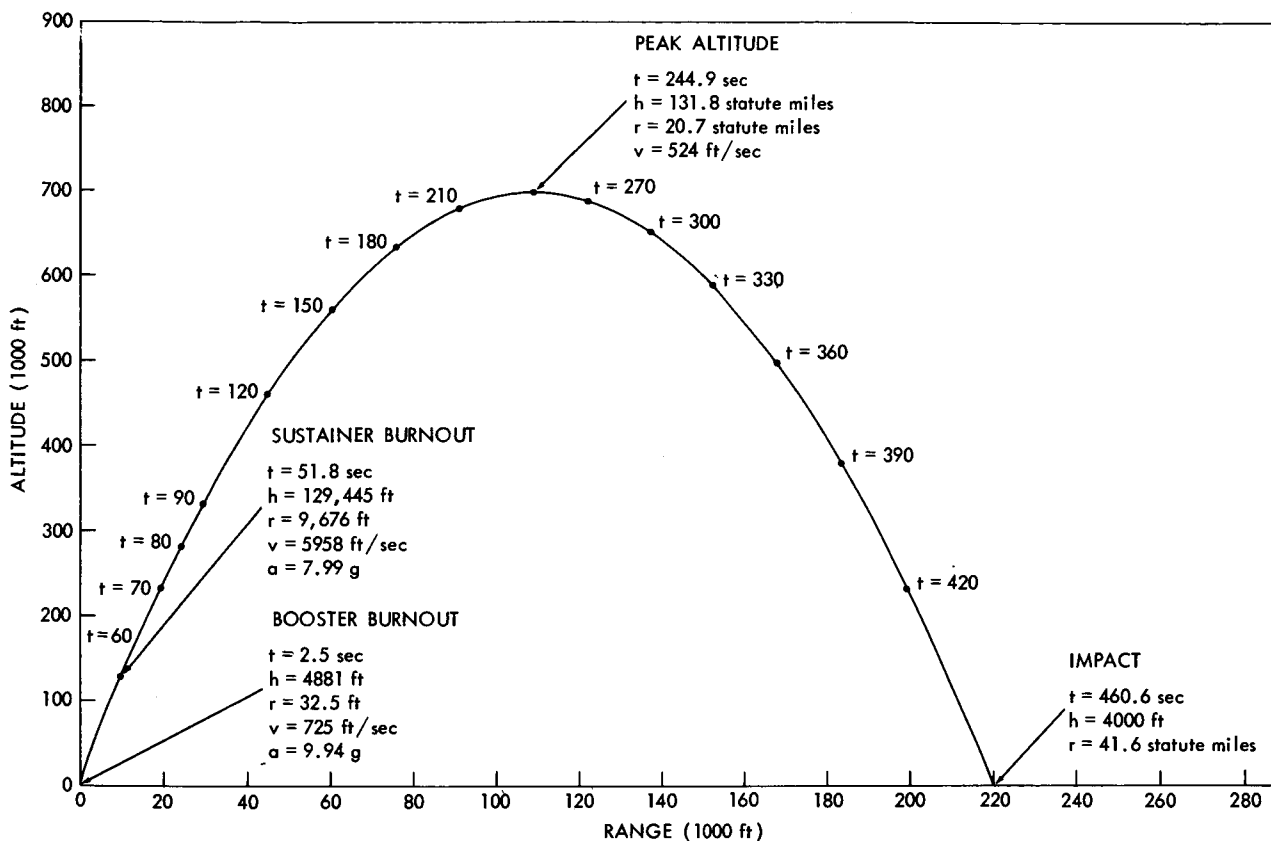
Figure 18—Expected performance trajectory for a rocket of similar weight and payload to that of 4.113 GA-GI.

films. At approximately 0.55 to 0.60 seconds, the sustainer flame apparently went out, but again became visible at 0.65 seconds and lasted until 0.70 seconds (note frames d, e, f, g in Figure 19). At this time, as indicated by color photographs, the smoke from a residual sustainer flame had become a dark reddish brown. When the rocket left the tower at 0.95 to 1.0 seconds, it was still emitting a dense cloud of reddish brown smoke. On the basis of its color and the characteristic odor present in the air, observers concluded that the smoke was rich in IRFNA (inhibited red fuming nitric acid).

Compare the normal flame in Figure 2 of Aerobee 4.67 NP with the flame in Figure 1 of NASA 4.113 GA-GI. The flame in Figure 1 is shorter but wider, and the booster is almost obscured from view by the dense smoke which starts well foreward of the booster. Normally, the booster fins are easily identifiable since the normal gray-white smoke comes from the booster. However, it is seen in Figure 1 that the smoke, instead of the normal orange flame, also came from the sustainer motor.

At approximately 2.5 seconds, the booster separated, after which the sustainer flame pulsated (alternate short flame, long flame, see Figure 20) at 10 cps and continued to burn with a reddish brown smoke that faded to a pale yellow-white at approximately 20 seconds. At approximately 25.05 seconds, a "puff" was observed. Other such puffs were observed at 25.4, 25.8, 26.3, 26.75,
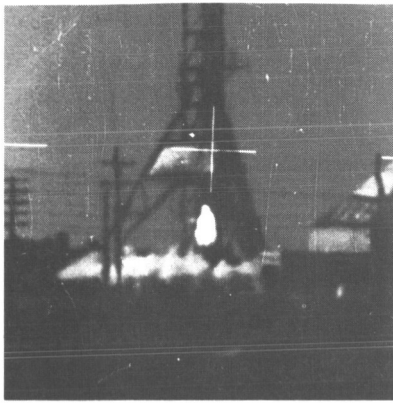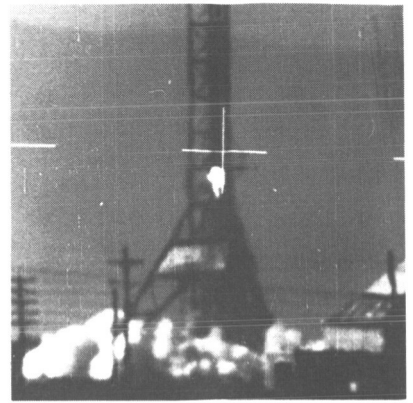
(a)   (b)   (c)
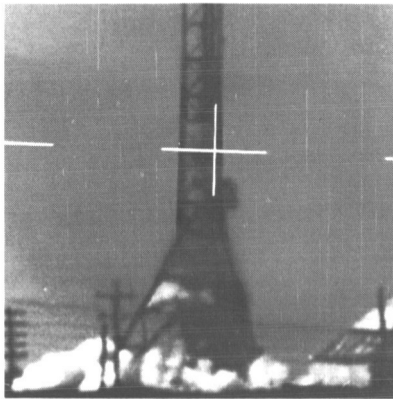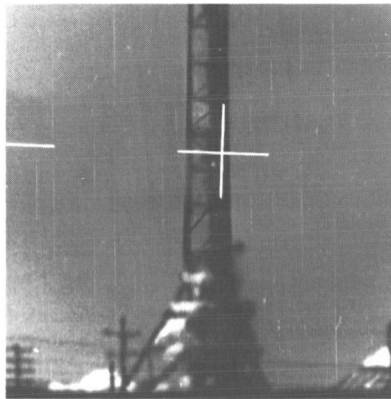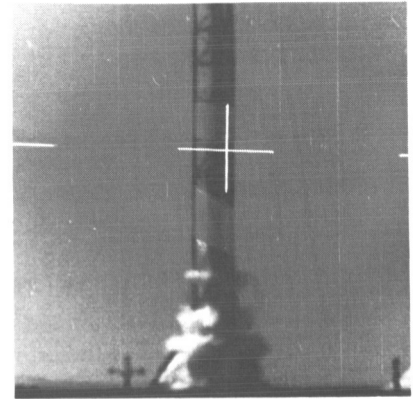
(d)   (e)   (f)
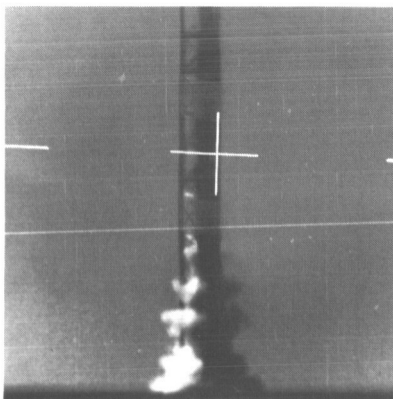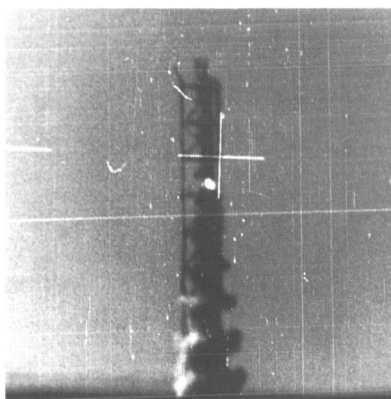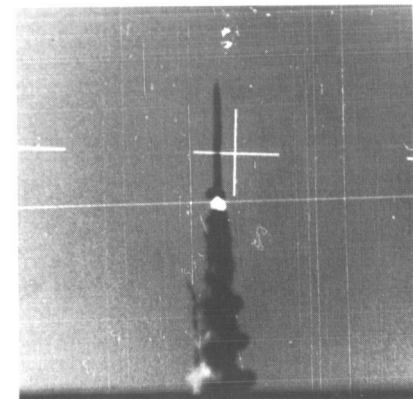
(g)   (h)   (i)

Figure 19—Sequence (20 fps) of NASA 4.113 GA-GI lift-off.
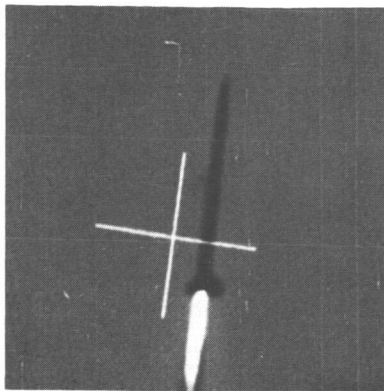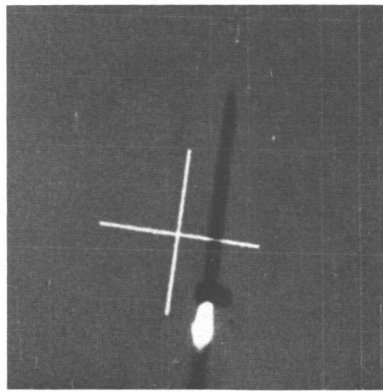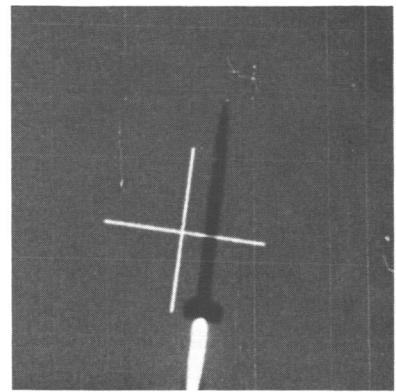
(a)   (b)   (c)

Figure 20—Sequence of pulsating flame.

and 27.2 seconds. Owing to the tracking angle of the camera loaded with color film, color photographs of the puffs were not taken. This is unfortunate since it is not possible to determine from the black-and-white tracking films whether the puffs were smoke or flame.

Figure 21a shows the tail can explosion at 27.4 seconds. Notice the angle of the rocket just after the explosion. Figure 21b is a view of the explosion from another tracking camera taken about 1/2 second later. Notice in this view also that the rocket is traveling almost sideways.
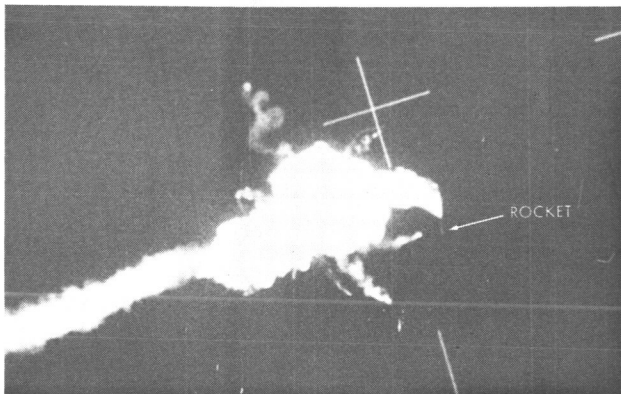
Figure 21a—Tail can explosion (+27.4 seconds).
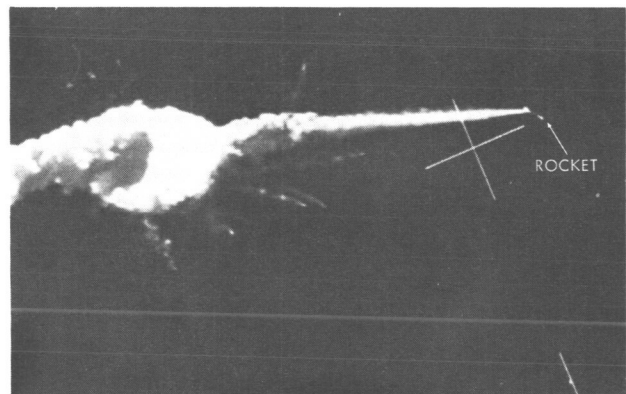
Figure 21b—Tail can explosion (film from another camera at approximately +28 seconds).

ANALYSIS OF RECOVERED ROCKET COMPONENTS

The recovered sustainer was returned to the U.S. Naval Ordnance Missile Test Facility, the helium pressure regulator was sent to the SGC for testing, and the aft end of the fuel tank and motor assembly, including the motor plumbing, were returned to GSFC for examination.

Postflight flow tests of the regulator at SGC revealed no flaws in the regulator or significant variations from preflight flow characteristics. No obstructions were observed in the helium, oxidizer, or fuel tanks, gas lines, propellant lines, shutoff valves, burst diaphragm housings, thrust chamber jacket (which was cut away for inspection), or the injector head.

The previously noted displacement of the O-ring from the pintle of the shutoff valve (Figure 8) could not be related in any way to the failure of 4.113 GA-GI but did point up a serious design deficiency in the fuel shutoff valve, used to conserve helium gas on attitude control system flights, which has been remedied by employing a new shutoff valve seat.

Also, it was observed that a portion of the chamber pressure tap and B-nut were missing (Figure 4). In addition to a break in the fuel line at the base of the fuel tank, a tap on the fuel coolant outlet line of the thrust chamber was missing. The squibs in the shutoff valves were unfired. The parts were submitted for metallurgical analysis.

The interior of the combustion chamber was examined. All fuel and oxidizer injector holes were open, and the hole for the chamber pressure tap was unobstructed and showed only a very small amount of errosion.

Tank ullages were volume-checked and found within specifications and no abnormalities were observed in gas or propellant diaphragms or orifices. The remaining portions of the gas and propellant diaphragms were examined to ascertain that only single thicknesses of material had been employed in manufacturing the portions that rupture. The check valve in the gas circuit functioned normally during postflight examination.

DISCUSSION AND CONCLUSION

The eyewitness reports, the noises, the exhaust odor, and the pulsating flame accompanied by the oxidizer-rich smoke cloud observed as the vehicle left the launch tower, coupled with onboard telemetering, radar, and theodolite data, clearly indicate that NASA rocket 4.113 GA-GI experienced unstable combustion conditions which continued until the tail can explosion at 27.4 seconds as a result of pressure built up by combustion gas and fuel. The other abnormalities during the flight are also the result of the malfunction occurring in the start transient.

A hard start can occur either if there is a fuel lead into the combustion chamber, or a significant delay in ignition (Appendix A gives a brief discussion of ignition phenomena). When either of these happen, high combustion chamber pressures are generated which can rupture parts of the thrust chamber. Pressures experienced during hard starts on test stand firings, for example, have been observed to be sufficient to cause extremely high chamber pressure through the fuel injector head—high enough, in fact, to blow out the pressure tap on the fuel line between the coolant jacket and the injector or to break the chamber pressure tap, both of which are believed to have happened on this flight. The burned aniline fuel residue on the fuel tank aft bulkhead and the outside of the thrust chamber, evident in Figures 3 and 4, presumably resulted from the flow of large quantities of fuel into the tail can section after the tap on the fuel line was blown out.

14

By reviewing similar hard start conditions on other flights (Appendix B describes an Air Force failure at Eglin AFB, 1960), and by discussing the results of test stand firings in which hard starts were observed, possible causes of a hard start in the Aerobee have been postulated:

1. Improper helium pressure regulation resulting in improper propellant tank pressurization and improper initial propellant flow rates.

2. Obstructions in propellant or gas lines, etc. causing an unbalanced flow of propellants.

3. Improper propellant contents and temperatures resulting in ignition lag.

4. Improper-sized gas or mixture ratio orifices.

5. Structural failures at normal working pressures.

6. Improper ullage affecting tank pressurization rates.

7. Improper burst sequence of propellant diaphragms.

8. Improper burst sequence of gas diaphragms.

9. Improper fuel bleed.

Of the above possible causes of a hard start all but three have been eliminated. Cause 1 was eliminated by the postflight flow tests and inspection at SGC. Cause 2 was eliminated by a post-flight visual inspection.

Cause 3 was eliminated since propellant contents and temperatures for this flight were within specifications, ruling out the possibility of ignition lag. Chemical analyses performed on both propellants before and after flight verified that propellant contents were within specifications. Temperatures of the propellants in the rocket tanks taken immediately after servicing were 62°F for the oxidizer and 72°F for the fuel. Thus no significant change could have taken place in propellant expansion or contraction (which would affect ullage and ultimately tank pressurization rates), as ambient temperature at lift-off was 62°F.

Cause 4 was eliminated by postflight measurements and inspection. Cause 5 was eliminated when a metallurgical investigation of the recovered rocket components concluded that the failure was not due to structural failure or manufacturing defect.

Cause 6, improper ullage, perhaps merits consideration in somewhat greater detail. An excessive ullage in the oxidizer tank would increase time required to pressurize the oxidizer which in turn could well cause a fuel lead into the combustion chamber. On the other hand, an insufficient ullage in the fuel tank might also cause a fuel lead-in through excessive tank pressure. Improper ullage can result from either a "buildup" of manufacturing tolerances, changes in propellant temperatures, or from improper servicing techniques. Some difficulty was experienced in the fueling operation of this flight, but was reported to have been remedied.

The possibility of improper ullage due to deviation from manufacturing tolerances has been ruled out by postflight volume measurement of recovered hardware. Improper ullage due to other factors is ruled out by the slight temperature variation from propellant servicing time to launch

time and visual assurance of three observers that the propellant tanks were properly loaded and good return flow was obtained through the "Y"-nozzles, used to fill the propellant tanks.

Thus, three significant possible causes, 7, 8 and 9, remain: a gas diaphragm bursting out-of-specification, a propellant diaphragm bursting out-of-specification, or an improper fuel bleed.

If a gas diaphragm breaks out-of-tolerance, a pressurization sequence occurs which could cause an improperly balanced flow of fuel and oxidizer and possibly a fuel lead-in. Likewise, if the propellant diaphragms burst out-of-tolerance, a fuel lead into the thrust chamber or excessive initial flow rates could cause a hard start. Since quality control measures for inspecting diaphragms require their total destruction, it is impossible to state that a particular diaphragm will not break at an improper pressure. Appendix C contains information on gas and propellant burst diaphragm tests conducted subsequent to the 4.113 GA-GI failure in order to substantiate the reliability of these diaphragms.

If the air is not properly bled out of the thrust chamber coolant jacket while the start slug is being inserted, the entrapped air acts as a compressible spring. A pressure surge, similar to a "water hammer" effect, could occur causing the fuel diaphragm to break early, allowing fuel to precede the oxidizer into the thrust chamber.

Although it is impossible to state conclusively which of the above conditions was definitely responsible for this failure, improper fuel bleed or propellant diaphragm failure is considered the most likely.

Gas diaphragm failure is considered the least likely of the causes of the malfunction which have not been positively eliminated because these diaphragms experience a very high gas pressure rise rate (greater than 70,000 psi/sec) to the working regulated pressure. Consequently an extreme manufacturing discrepancy would be required to cause a significant difference in diaphragm bursting time. The burst pressure of one of the diaphragms would probably have to be greater than the regulated pressure for this to exist.

As a result of the failure of NASA flight 4.113 GA-GI measures have since been taken to avoid a recurrence:

1. Increased checks are being performed during rocket buildup to assure that the various potential causes of a hard start (itemized above) cannot exist.

2. Increased quality control is being maintained in the production of propellant and gas burst diaphragms (Appendix D).

3. Increased care is being exercised in propellant servicing especially in bleeding the thrust chamber jacket by flowing an increased quantity of fuel through the jacket and out the bleed fitting. There does, however, exist some doubt in the authors' opinion as to the adequacy of this technique. Other techniques for assuring that all air is removed from the jacket are being investigated.*

*At the time of printing this note, a bleed technique utilizing quick disconnects is being incorporated into the rocket servicing procedure.

ACKNOWLEDGMENTS

BIBLIOGRAPHY

1. Adelman, B. R., "Apparatus for Laboratory-Scale Determination of Ignition Lag of Spontaneous Liquid Rocket Propellants," Jet Propulsion Laboratory, California Institute of Technology, Feb. 23, 1961.

2. Chalfant, C. P., "Start Transient Evaluation of the Aerobee 150A Propulsion System," Supp. Report No. 1640A, Aerojet General Corp., Azusa, Cal., August 1960.

3. Cox, R. B., "Static Test Firing of Aerobee Sounding Rocket Engines," Aerojet General Corp., Azusa, Cal., Jan. 27, 1955.

4. Griffin, D. M., and Clark, E. M., "Effect of Low-Temperature and Sub-Atmospheric Chamber Pressure on Ignition Delay of RFNA Aniline-Furfuryl Alcohol Propellant Systems," Progress Report No. 1-78, Jet Propulsion Laboratory, California Institute of Technology, Sept. 9, 1951.

5. Krenzon, V. A., Migdal, N. T., Rumbold, S. G., and Stone, M. S., "Aerobee Investigation Report No. 326FR-2," Space General Corp., El Monte, Cal., Sept. 1963.

6. Migdal, N. T., "Performance Verification Tests of the Aerobee 150 (Model AGVL-0113F)," Aerojet General Corp., Azusa, Cal., Oct. 6, 1958.

7. Ring, E., "Rocket Propellant and Pressurization Systems," Englewood Cliffs, N.J.: Prentice-Hall, Inc., 1964.

RFNA—furfuryl alcohol, were thoroughly investigated to determine their ignition-lag behavior under various conditions. Based on the results of these studies, parameters such as stream velocity, propellant-tank pressure, and mixture ratio, which may have some effect on ignition lag, were standardized and subsequent tests on other systems were performed under one set of conditions to facilitate comparison of results.

Although the absolute values of the ignition lags determined in the laboratory-scale apparatus may not be identical with those measured in actual rocket motors with widely variant conditions of propellant injection, chamber dimensions, mixing parameters, and chemical factors, the data should prove valuable in establishing a table of relative values of ignition lag to be expected with given propellant systems under operating conditions.

The chemical factors involved in ignition with propellant systems employing nitric acid as the oxidizer may be broken down into three groups: *neutralization reactions, nitration reactions, and oxidation reactions*. These reactions may occur singly or simultaneously in either the vapor or the liquid phase; the one which occurs most slowly would probably control the ignition-lag characteristics of the system, though it would not necessarily control the steady-state combustion. Considering the temperatures involved, it seems probable that before visible flame appears, a portion of the mixed propellants has been vaporized although the controlling reactions which produce the necessary heat probably occur in the liquid phase.

Motor Tests

To arrive at the most suitable ANFA and RFNA combinations, over five hundred individual tests were made by JPL with the ignition-lag motor completing a preliminary study of ignition lag as a function of various motor operating conditions.

Representative data of the results are presented below:

Aniline-RFNA

Several successful tests were made; however, in the majority of tests, hard starts were experienced which blew the nozzle off the motor. Because of the severe conditions to which the motor was subjected by this fuel system, reproducibility from test to test was poor; therefore no attempt was made to continue testing with aniline alone as fuel. The difficulty was the result of a pressure surge accompanying ignition in this motor which reaches a maximum value greater than the feed pressure. Hence an oscillating condition can occur in which ignition causes a cessation in the flow of propellants which in turn allows the flame to be extinguished in the chamber. After this occurrence the measurement of ignition-lag phenomena in the motor may be repeated. These subsequent ignition-lag measurements are designated as secondary, inasmuch as temperature conditions, etc. in the motor are changing over the period of a given start.

Ignition Characteristics of Various Liquid Propellants

A brief discussion of the ignition characteristics of aniline furfuryl alcohol (ANFA), red fuming nitric acid (RFNA), which is of particular interest in connection with "hard" starts is presented for background information.

The following descriptions are based on JPL Progress Reports 20-138 and 9-30 (References A1 and A2).

Introduction

The term spontaneous, when applied to rocket fuel systems, means self-igniting; however, spontaneous ignition should not be considered an instantaneous process. For a fuel system to be spontaneous, sufficient heat must be liberated through chemical reaction to elevate the temperature of the system to the point where kindling, or ignition, will occur. Therefore, a finite period of time will elapse between the moment of mixing and the moment at which ignition occurs. This period is arbitrarily designated as ignition lag. It is evident that ignition lag, so defined, is not in itself a fundamental quantity, but is dependent on many physical factors such as the conditions of mixing, initial temperature, and the geometrical configuration of the system, as well as the chemical reactivity of the fuel components.

It is generally recognized that the starting characteristics of liquid-propellant rockets are affected by the ignition lags of the propellant systems employed. This has led to the development of equipment to measure ignition lags of rocket propellant systems accurately under conditions analogous to those encountered in motor operations.

A comprehensive study of ignition lag should be subdivided into two basic categories which must be attacked separately. Because both physical and chemical factors are involved in the kinetics of spontaneous ignition, it becomes desirable to study ignition lag first as a function of motor design and operating conditions, and second as a function of the chemical nature of the fuel systems independent of the mechanics involved in practical operation. This circumstance can only be approached, inasmuch as it is practically impossible to mix two spontaneous reactants without imposing the conditions of mixing upon the reaction; however, the chemical aspect could be studied by holding constant the various physical conditions in a given system. It is possible that information obtained through these two separate approaches can ultimately be correlated to form a more complete picture of the general problem.

The present discussion deals with the results of an initial series of tests performed utilizing laboratory-scale apparatus. The more common propellant systems, including RFNA-aniline and

RFNA—furfuryl alcohol, were thoroughly investigated to determine their ignition-lag behavior under various conditions. Based on the results of these studies, parameters such as stream velocity, propellant-tank pressure, and mixture ratio, which may have some effect on ignition lag, were standardized and subsequent tests on other systems were performed under one set of conditions to facilitate comparison of results.

Although the absolute values of the ignition lags determined in the laboratory-scale apparatus may not be identical with those measured in actual rocket motors with widely variant conditions of propellant injection, chamber dimensions, mixing parameters, and chemical factors, the data should prove valuable in establishing a table of relative values of ignition lag to be expected with given propellant systems under operating conditions.

The chemical factors involved in ignition with propellant systems employing nitric acid as the oxidizer may be broken down into three groups: *neutralization reactions, nitration reactions, and oxidation reactions*. These reactions may occur singly or simultaneously in either the vapor or the liquid phase; the one which occurs most slowly would probably control the ignition-lag characteristics of the system, though it would not necessarily control the steady-state combustion. Considering the temperatures involved, it seems probable that before visible flame appears, a portion of the mixed propellants has been vaporized although the controlling reactions which produce the necessary heat probably occur in the liquid phase.

Motor Tests

To arrive at the most suitable ANFA and RFNA combinations, over five hundred individual tests were made by JPL with the ignition-lag motor completing a preliminary study of ignition lag as a function of various motor operating conditions.

Representative data of the results are presented below:

Aniline-RFNA

Several successful tests were made; however, in the majority of tests, hard starts were experienced which blew the nozzle off the motor. Because of the severe conditions to which the motor was subjected by this fuel system, reproducibility from test to test was poor; therefore no attempt was made to continue testing with aniline alone as fuel. The difficulty was the result of a pressure surge accompanying ignition in this motor which reaches a maximum value greater than the feed pressure. Hence an oscillating condition can occur in which ignition causes a cessation in the flow of propellants which in turn allows the flame to be extinguished in the chamber. After this occurrence the measurement of ignition-lag phenomena in the motor may be repeated. These subsequent ignition-lag measurements are designated as secondary, inasmuch as temperature conditions, etc. in the motor are changing over the period of a given start.

Furfuryl Alcohol-RFNA

Because hard starts had been experienced with aniline-RFNA in the present motor setup, it was decided to use furfuryl alcohol, a smoother starting fuel than aniline, in the same motor rather than varying the motor configuration. Smooth starts were obtained using furfuryl alcohol-RFNA with the same injectors and motor chambers used with aniline-RFNA.

Furfuryl Alcohol-Aniline Fuel Mixtures

In order to determine the effect on ignition lag of variations in the concentration of furfuryl alcohol in aniline (when this fuel mixture is used with RFNA), a series of tests was made in which the concentration of furfuryl alcohol in aniline was varied from 10 to 100 percent by volume. For these tests the motor system was not changed from the previous conditions. The ignition lags obtained are shown in Figure A1.

Effect of Mixture Ratio on Ignition Lag

Motor tests were made to determine the effect of mixture ratio on ignition lag. Furfuryl alcohol and RFNA again were used as the propellant system. A single pair of injectors was used, and the mixture ratio was varied by varying the tank feed pressures separately on the two propellant tanks. Total propellant flow rates were kept approximately constant by increasing the flow rate of one component while decreasing the other (Figure A2).

Ignition lag increased when the motor was operated at very high and very low mixture ratios. The starts were audibly rougher at very low mixture ratios.

Effects of Temperature on Ignition Lag

No direct tests were made to determine the effect of temperature on ignition lag; however, several effects were observed which were attributed to temperature. Considering ignition lag from a purely chemical standpoint, it would be assumed that increasing the temperature of the reactants would increase the rate of reaction and hence would decrease ignition lag.
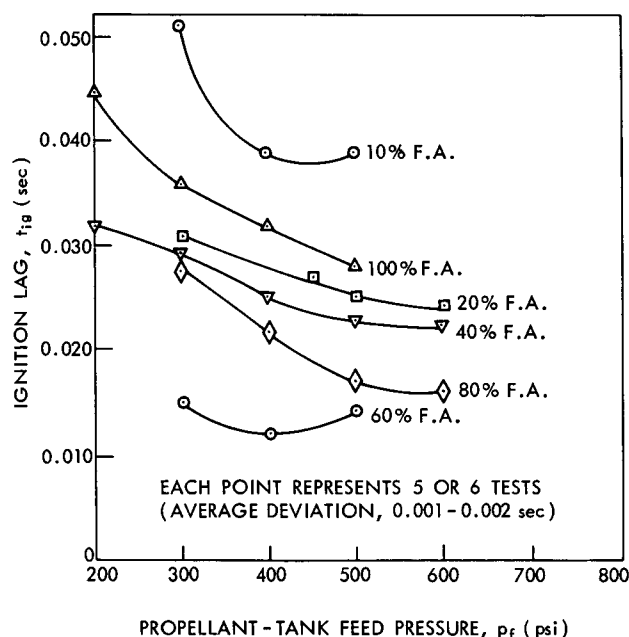
Figure A1—Ignition lag on various furfuryl alcohol-aniline mixtures with RFNA.
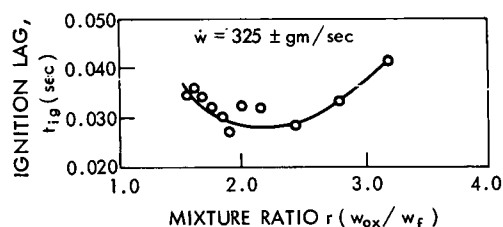
Figure A2—Ignition lag as function of mixture ratio.

Significance of Constant Ignition Lag at Various Mixture Ratios

The ignition lag of RFNA-aniline and RFNA-furfuryl alcohol systems is essentially constant over a wide range of mixture ratios. If one considers the equation

$$P_{max} \leq \frac{C\Gamma^2}{\gamma V_{cg}} \, \dot{\omega} \, c*^2 \, t_i \, ,$$

(A1)

where

$c*$ = characteristic velocity (ft/sec)

C = constant form to compensate for nonideality of combustion gases in the equation
$PV = CnRT$

g = gravitational constant 32.2 ft/sec^2

n = number of moles of gas present

P_{max} = maximum transient chamber pressure at ignition (psia)

R = universal gas constant

t_i = ignition lag (sec)

V_c = chamber volume (cu in.)

γ = ratio of average specific heats of exhaust gases

$\Gamma = \left(\frac{2}{\gamma+1}\right)$

$\dot{\omega}$ = average mass rate of flow of propellants before ignition (lb/sec),

which defines the maximum transient pressure upon ignition (assuming no mass flow through the nozzle preceding ignition), it may be seen that the term $C\Gamma^2/\gamma V_{cg}$ is essentially constant for any given propellant system. The derivation and discussion of this equation are given in Reference A3.

The term which is the average weight rate of flow of the propellant before ignition may also be made constant for any given test. Thus Equation A1 may be written

$$P_{max} \leq K \, c*^2 \, t_i \, ,$$

(A2)

where K is a constant term, the value of which depends upon the propellant system used and the propellant flow rates employed. The fact that for certain propellant combinations the ignition lag is constant over a wide range of mixture ratios allows Equation A2 to be still further simplified to

$$P_{max} \leq K' \, c*^2 \, .$$

(A3)

(where $K' = Kt_i$) for the range of constant t_i in those systems.

If $c*^2$ for any bipropellant system is plotted vs. percentage of oxidizer, a curve is obtained which has a maximum value and returns to a low value at 100 percent oxidizer. Values of the mixture ratio plotted along the abscissa of such a curve form a logarithmic scale. A representative

curve of this type is shown in Figure A3 for the WFNA-furfuryl alcohol system. It should be noted that the maximum value of the square of the characteristic velocity falls on the fuel-rich side of the stoichiometric mixture ratio. Also at no point on the fuel-rich side of the stoichiometric mixture ratio in the region of stable ignition is the value of $c*^2$ less than that at the stoichiometric point. However, at every point on the oxidizer-rich side, the square of the characteristic velocity is less than that at the stoichiometric mixture ratio. It may therefore be concluded that, for propellant systems in which the ignition lag is constant over a wide range of mixture ratios, minimum transient chamber pressures at ignition will be obtained if motors are started on the oxidizing side of the stoichiometric point.
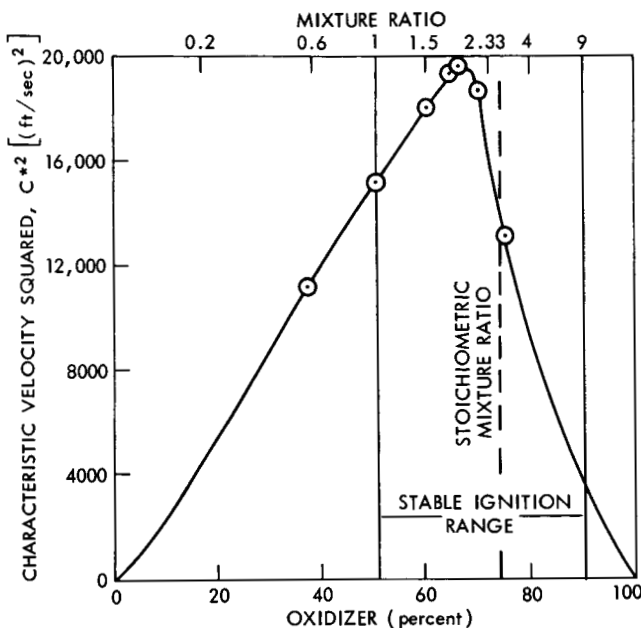
Figure A3—Characteristic velocity squared vs. percentage of oxidizer and mixture ratio for WFNA-furfuryl alcohol system.

Conclusions

From the investigation of ignition-lag characteristics of various propellant systems with the laboratory-scale apparatus, the following conclusions may be drawn:

1. There is good agreement between ignition-lag data obtained in the test motor and in the laboratory-scale equipment.

2. The ignition lag of RFNA-aniline and RFNA-furfuryl alcohol systems is essentially independent of mixture ratio over a wide range.

3. Experiments utilizing the laboratory-scale apparatus show definitely that both the chemical composition and the structure of organic fuels affect the ignition lag of spontaneous liquid-propellant systems utilizing them.

4. Since the maximum transient chamber pressure at ignition depends upon the square of the characteristic velocity, lower instantaneous pressures and hence smoother starts should be obtained by starting rocket motors on the oxidizing side of the stoichiometric mixture ratio. This conclusion applies to those systems whose ignition lags are substantially independent of mixture ratio.

REFERENCES

A1. Adelman, B. R., "A Study of Ignition-Lag Characteristics of Some Liquid Rocket Fuels with Red Fuming Nitric Acid, Including Additives to the Oxidizer," Progress Report No. 20-138, Jet Propulsion Laboratory, California Institute of Technology, April 18, 1951.

A2. Griffin, D. M., "A Program for the Study of Ignition Laboratory of Spontaneous Liquid Rocket Propellants," Jet Propulsion Laboratory, California Institute of Technology, May 17, 1949.

A3. Adelman, B. R. and Burnett, R., "Apparatus for Laboratory-Scale Determination of Ignition Lag of Spontaneous Liquid Rocket Propellants," Jet Propulsion Laboratory, California Institute of Technology, Sept. 15, 1950.

Appendix B

Launch Report of Hughes Aerobee 300 (S/N AF-49), 18 August 1960, Eglin Air Force Base*

Aerobee 300 S/N AF-49 was launched from Eglin Air Force Base, Site A-11, on 27 July at 14:03 CST. The rocket flight was terminated at approximately 25 seconds by an explosion in the second stage. The object of the experiment was to obtain AM, UHF communications at high altitude.

The vehicle was the fourth in a series of six for Hughes Aircraft Co. who is building the payload. For this flight, the payload had been modified to include telemetry and various changes in the transmitter. Telemetry monitored several skin temperatures, transmitter voltages and nose cone pressure. The 8" diameter of the payload had been extended to 37-1/4" and a 2-7/8" cylindrical section had been inserted in the nose cone. The transmitter had been rescheduled to remain silent for 1/2 second, broadcast a carrier signal for 1/2 second, and then a modulated signal for 1/2 second. The payload was pressurized to 18 psig with Freon gas, which was used for cooling the transmitter.

The rocket consisted of a 2.5 KS 18,000 solid booster, and AJ11-21 sustainer and a 1.8 KS 7800 solid third stage. The second stage contained a DPN-41 range safety beacon and a DRW-11 command cut-off system.

Buildup of this unit was first completed in March. The launch date was postponed and the sustainer was returned to storage. On 22 July, the vehicle was removed from storage and subjected to an abbreviated series of checks in preparation for launch on 27 July. The forward end of the third stage shell grain was cemented in place with an epoxy resin. Installation in the tower was accomplished on 26 July after completion of the horizontal checks. A high pressure helium system leak check was completed satisfactorily on the same day. Fuel servicing began following this check and was completed without incident. On 27 July, preliminary payload and beacon checks were completed prior to acid servicing. The third stage was removed for beacon rework and reinstalled. Checks included firing circuit operation. Acid servicing was accomplished with no difficulty and no spillage occurred. After last firing circuit and beacon checks, the igniters and squibs were installed and connected. Pressurization of the helium system was completed to 3450 psig and held until firing at 1404 Central Standard Time.

The flight terminated at 25 seconds when the second stage failed. Examination of the photographs revealed erratic burning of the second stage for the entire flight time. Slow motion film of the rocket traveling through the tower, showed irregular burning of the second stage, with changes

in the color of the exhaust. The Contraves film shows intermittent burning starting at 4 seconds with a change in the color of the exhaust from white to dark gray. This continued with intermittent puffs of white smoke, until 25 seconds. During this time, the exhaust flame was not visible. At 25 seconds an explosion took place toward the aft end of the second stage. Tracking of the third stage continued until impact, at which time telemetry was lost at 100 seconds. Tumbling of the package was observed. Radar was lost at 30 seconds, at which time the vehicle was 1000 yards offshore and at an altitude of 15,000 feet. The vehicle flight path was on the center of the range. Payload pressure remained constant at 2 psig and only a small rise in payload skin temperature was observed.

Appendix C

Aerobee 150 Propulsion System Flow Tests

As a result of the failure of flight 4.113 GA-GI, several individual flow tests were conducted by the Space General Corporation to investigate the effects of various Aerobee 150 propulsion system components under operating conditions. A description of these tests and the conclusions derived by the Space General Corporation follows.*

Gas Burst Diaphragm Tests

Aerobee gas burst diaphragms (P/N 2-003452), used in fuel and oxidizer lines, were tested to answer the following questions:

(1) Do the diaphragms burst within the acceptance test range?

(2) Do the oxidizer and fuel diaphragms break at the same pressure when installed in the actual system?

(3) What is the time delay between fuel and oxidizer diaphragm bursting under actual flight conditions?

(4) Can the burst pressure of the diaphragm be changed through deformation caused by mishandling?

(5) Does the nominal 100 psig leak test pressure have any effect on the diaphragm burst pressure?

Table C1 describes a series of sixteen tests conducted in a setup simulating the actual flight configuration. This included regulator, gas manifold, check valve, fuel and oxidizer orifice, and simulated downstream ullage. Twenty-one diaphragms were tested, providing answers to all the pertinent questions as follows:

(1) Tests 5, 11, 15, and 16 indicate that the diaphragms break between 200 and 300 psi, as specified for acceptance testing at a low pressure rate of rise. All other tests were run at high pressure rates of rise, as experienced in the actual system, with resulting burst pressures of 310 to 375 psi.

(2) Tests 8 and 9 were run with deformed diaphragms showing no significant effect on burst pressure.

Table C1

Aerobee Gas Burst Diaphragm Tests.
(Burst Diaphragm P/N 2-003452)

Test	Diaphragm	Pressure Rise Rate (psi/sec)	Burst Pressure (psig)	Remarks
1	Oxidizer	70,000	330	Fuel side capped; diaphragm shattered
2	Oxidizer	70,000	325	Fuel side capped; diaphragm shattered
3	Oxidizer	70,000	320	Fuel side capped; diaphragm shattered
4	Oxidizer	70,000	350	Fuel side capped; diaphragm shattered
5	Oxidizer	425	275	Fuel side capped; clean diaphragm break
6	Fuel	100,000	350	Oxidizer side capped; diaphragm shattered
7	Fuel	150,000	320	Oxidizer side capped; diaphragm shattered
8	Fuel	150,000	310	Oxidizer side capped; diaphragm shattered; used deformed diaphragm
9	Fuel	150,000	325	Oxidizer side capped; diaphragm shattered; used deformed diaphragm
10	Fuel	150,000	320	Oxidizer side capped; diaphragm shattered
11	Fuel	16	250	Oxidizer side capped; clean diaphgram break
12	Fuel	100,000	325	Both diaphragms installed; shattered
	Oxidizer		375	
13	Fuel	150,000	330	Both diaphragms installed; shattered
	Oxidizer	100,000	370	
14	Fuel	100,000	340	Both diaphragms installed; shattered 100 psi leak test applied
	Oxidizer	94,000	350	
15	Fuel	106	260	Both diaphragms installed
	Oxidizer	106		Clean diaphragm break; 100 psi leak test applied
16	Fuel	650	290	Both diaphragms installed
	Oxidizer	650	280	Clean diaphragm break; 100 psi leak test applied

(3) For tests 14, 15, and 16, the 100 psig leak test was simulated prior to burst. No significant effect on burst pressure was realized.

From the available test data the following observations were made:

(1) The diaphragms break within the range of 200 to 300 psi as required for batch acceptance.

(2) There is no significant difference in the fuel and oxidizer diaphragm burst pressure when tested under actual flight conditions either separately or in combination.

(3) When both diaphragms are burst together there is approximately a 1 to 2 millisecond delay between bursts with the fuel diaphragm breaking first. This has been attributed to the existence of the check valve in the oxidizer circuit upstream from the diaphragm.

(4) Tests 8 and 9 indicate that no change in burst pressure is experienced when the diaphragms have obvious scratches, nicks, and dents.

(5) The application of 100 psi on the diaphragms for 60 seconds had no apparent effect on the subsequent burst pressures.

A preliminary statistical evaluation of the data in Table C1 is given in Table C2 below.

Table C2

Statistical Summarization of Data in Table C1.

Test Category	Sample Size	Average Pressure (psig)	Standard Deviation	
			(psig)	(percent)
All tests	20	319.2	34.0	10.6
Excluding low pressure rate-of-rise tests	15	335.3	19.6	5.8
Low pressure rate-of-rise rests	5	271.0	16.0	5.9

By excluding the low pressure rate-of-rise tests for helium disc burst pressures, the relative variance for the test lot is reduced. As the relative variances for the excluded items and the remaining are of the same order of magnitude, it is reasonable to assume that they came from similar populations but are independent.

Using the data with the low pressure rise rates excluded, a three-sigma limit about the average burst pressure, $\bar{P}$, yields a helium disc burst pressure of $P_B = 336 \pm 60$ psig. This is higher than the current design limits, indicating that some production changes should be effected. An estimate of the probability of exceeding a given design range can be calculated for an entire lot produced at the same time if some members of the lot are sampled. This reliability estimate, with a

corresponding confidence limit, depends upon the values assigned to the upper and lower allowable burst pressures.

A tightening of production control is desirable. This could be effected by a tightening of the burst range specification on working drawings, with an average value for bursting pressures, P_B, near 250 psig.

Propellant Burst Diaphragm Tests

Several Aerobee 150 propellant burst diaphragms (P/N 2-045074) were tested to determine burst pressures, rise rates, effects of mishandling, and effects of leak test pressures. Only six samples were taken (Table C3). However, the consistency of the burst pressures indicated that sufficient data were available to dispel any major problem areas. The results of these tests were as follows:

Table C3

Propellant Burst Diaphragm Tests.
(Burst Diaphragm P/N 2-045074)

Test	Pressure Rise Rate (psi/sec)	Burst Pressure (psi)	Remarks
1	100	47	
2	100	57	10 psi leak test pressure applied
3	3	48	
4	3	52	10 psi leak test pressure applied
5	300	55	
6	300	55	Mishandled diaphragm

(1) The specified burst pressure range of 45-80 psi at a rise rate of 200 psi/min was met in two tests, and tests at higher rise rates were also within this pressure range. There does appear to be a slight trend for the burst pressure to increase after the diaphragm has been subjected to the 10 psi leak test. The mishandling of one diaphragm did not affect the burst pressure.

(2) With only two propellant discs being burst at each of the three pressure rise rates, estimates of variance of burst pressure are not conclusive. Taking the values to be independent, the combined data gives, at a three sigma limit, P_B = 52.7 ± 16.8 psig. The relative variance for the samples is 5.6 percent, which compares favorably with other burst disc tests. The reliability estimations for the propellant burst discs are dependent upon specified allowable burst pressure limits.

Fuel Shutoff Valve Tests

A series of tests were conducted on fuel shutoff valves (P/N 2-007870) in order to investigate any contribution of this part to Aerobee propulsion system failures, especially that of flight NASA 4.113 GA-GI, following which an "O"-ring was found in the burst diaphragm cage. The valve was modified by installing a screw in the valve cap (P/N 2-037093) which would allow the piston-seat assembly to be held in various positions in the flow stream prior to the beginning of the tests. Table C4 provides the results of tests conducted with valve assembled per drawing and seat (P/N 2-031078) finger tight. The valve was flowed with a 450-psig back pressure.

Table C4

Fuel Shutoff Valve Tests with Seat Finger Tight.

Test	Pressure Drop (psi)	Flow Rate (lb/sec H_2O)	O-Ring	Valve Piston Position (in.)	Remarks
1	6.9	3.96	In place	0.0	Valve in locked position; full open
2	6.9	3.96	Lost		Seat unscrewed and fell off after approximately 3 minutes flow time. Valve did not shut off.
3	6.3	3.96	In place	0.0	Valve in unlocked condition; full open; seat torqued to 18 in-lb.
4	12.0	5.49	In place	0.0	
5	18.5	6.89	In place	0.0	

Table C5 provides the results of tests conducted with seat torqued to 20 in-lb and set screw (at top of valve cap) screwed down one turn and held in place for each succeeding test.

Table C5

Fuel Shutoff Valve Tests with Seat Torqued 20 in-lb.

Test	Pressure Drop (psi)	Flow Rate (lb/sec H_2O)	O-Ring	Valve Piston Position (in.)	Remarks
1	12.5	5.7	In place	0.0	Valve in unlocked condition
2	12.7	5.7	In place	0.031	
3	13.1	5.7	In place	0.062	
4	13.5	5.7	In place	0.093	
5	13.8	5.7	In place	0.124	
6	14.1	5.7	In place	0.155	
7	14.5	5.7	In place	0.186	
8	15.0	5.7	In place	0.217	
9	15.6	5.7	In place	0.248	
10	16.0	5.7	In place	0.279	
11	16.7	5.7	In place	0.310	
12	18.5	5.7	Lost	0.341	O-ring came off seat
13	19.5	5.7	Off	0.372	
14	21.0	5.7	Off	0.408	
15	23.0	5.7	Off	0.434	
16	25.0	5.7	Off	0.465	
17	28.2	5.7	Off	0.496	
18	32.6	5.7	Off	0.527	
19	40.0	5.7	Off	0.554	

Table C6 provides results derived from tests conducted with seat finger loose.

Table C6

Fuel Shutoff Valve Tests with Seat Finger Loose.

Test	Pressure Drop (psi)	Flow Rate (lb/sec H_2O)	O-Ring	Valve Piston Position (in.)	Remarks
1	13.0	5.7	In place	0.0	Valve in locked position
2	13.0	5.7	In place	0.244	Distance unscrewed in 1 minute
3	14.0	5.7	In place		
4	14.5	5.7	In place		
5	15.0	5.7	In place		
6	16.0	5.7	In place	0.307	Distance unscrewed in additional 2 minutes. Total flow time 3 minutes. Seat did not come off. 1-1/4 threads holding seat to piston

Table C7 provides the results of a test which was conducted with the valve locked and seat backed off one turn.

Table C7

Fuel Shutoff Valve Tests with Valve Locked, Seat Backed Off One Turn.

Test	Pressure Drop (psi)	Flow Rate (lb/sec H_2O)	O-Ring	Valve Piston Position (in.)	Remarks
1	—	5.7	In place	0.0	Start of flow
2	—	5.7	In place	0.308	Total time 3 minutes. 1-1/4 thread holding seat to piston; same as prior test.

A final test was conducted to determine if the seat (torqued to 20 in-lb) would return to the full open position or shutoff as the adjustment screw forced the seat into flow stream. Results of this test show the seat returned to full open through all settings from zero or full open position to 0.554 inches where the valve was almost closed. The seat had a total travel of 0.554 inches toward the closed position at the conclusion of the test.

Three significant conclusions were derived from these tests concerning full shutoff valves.

(1) The valve will not change the propulsion system flow characteristics when the seat is torqued to 18-20 in-lb.

(2) Even when the seat comes loose (valve locked or unlocked condition), the valve will not shut off.

(3) The maximum increase in valve pressure drop of 12.5 to 40 psi is not sufficient to cause a propulsion system failure.

All test results on gas burst diaphragms, propellant burst diaphragms, and fuel shutoff valves indicate that each component functions in the system as designed.

Appendix D

Aerobee Burst Diaphragm Acceptance Test Plan

The test procedure for vendor testing of Aerobee 150 burst diaphragms is performed in accordance with Space General Corporation Drawing No. 2-045074. This procedure requires the bursting of two of a lot of twelve assemblies at a pressure rate rise of 200 psi/min. Any burst pressure beyond the specified range of 45-80 psi requires rejection and rework of all assemblies made from the same material as the unacceptable burst diaphragm.

At the time of the failure of NASA flight 4.113 GA-GI, the vendor tests were the only ones performed. As a result of this flight failure, an in-house vendor acceptance test plan was formulated. The following vendor test plan is now applicable to all Aerobee burst diaphragms.

Introduction

The following plan describes an acceptance program based on MIL-STD-414 and ARGMA sampling criteria. The tests will be performed at SGC by SGC personnel. This plan will supplement the tool-proofing sampling plans now in effect, and will increase control over the quality of incoming diaphragms. The sampling plan will assure .9985 reliability for critical tolerance limits and a .996 reliability for less critical limits, e.g., lower limit of the oxidizer burst diaphragm. After a sufficient sample has been accumulated the program will convert from MIL-STD-414 to ARGMA, which will allow a 50 percent reduction in the required sample size.

Burst Pressure Limit Criteria

The critical limits for the fuel and oxidizer diaphragms are set to assure at least a .9985 probability that the differential burst pressure is not less than 25 psi. The less critical limit will assure a reliability of .996 that the fuel diaphragm burst pressure will not exceed the limits of the helium system and that the oxidizer diaphragm will survive the leak checks. The sampling plan will assure a .996 reliability that both the helium and propellant diaphragms burst within the functional limits.

Propellant Valve Assembly Diaphragms (150A P/N 1103290-1, -3)

The nominal values of the fuel and oxidizer burst diaphragms are stated to be 325 ● 10 and 200 ± 10 psig (160 ● 10 in system), respectively. The critical limit for the oxidizer diaphragm will be 250 psig and the critical limit for the fuel diaphragm will be set at 275 psig. The less critical limit of the fuel disc will be set at 375 psig (i.e., 55 psi less than

33

the estimated minimum helium pressure of 430 psig). The less critical limit for the oxidizer diaphragm will be set at 150 psi.

Helium Burst Diaphragms (150/150A P/N 2-003452)

A conservative estimate of minimum regulated helium pressure is 430 psig. Nominal drawing tolerances are 250 ± 50 psig. Functional limits of 250 ± 125 psig will allow a 55 psi differential between the minimum helium pressure and the burst pressure and a 25 psi differential for the 100 psig leak check.

Propellant Diaphragm (150 P/N 2-04574)

These diaphragms have a specified nominal burst pressure of 50 psig. The upper functional limit will be 75 psig and the lower limit will be 25 psig to protect against the 10 psig leak test. The drawing and functional acceptance limits for each diaphragm are presented in Table D1.

Table D1

Propellant Diaphragm Burst Limits.
(in psi)

Part		Drawing Limits	Acceptance Limits
Fuel Diaphragm	(1103290-3)	325 ± 10	325 ± 50
Oxidizer Diaphragm	(1103290-1)	200 ± 10	200 ± 50
Helium Diaphragm	(2-033452)	250 ± 50	250 ± 125
Propellant Diaphragm	(2-045074)	45 – 80	50 ± 25

Acceptance Test Plan (MIL-STD-414)

Lot Definition

A lot will be defined as the set of diaphragms made in one run from a single sheet by a single operator, on a single machine. Manufacture of the diaphragms will be controlled by the sampling plan given on each drawing. The SGC acceptance program will supplement these sampling plans and will be used to determine and control the reliability of the diaphragms.

Sample Size

A sample will be drawn at random from each lot using Table D2. Randomization can be achieved by numbering discs consecutively as they are produced and then drawing from a table of random digits the numbers of the discs for each test.

34

The diaphragms will be acceptance tested in a fixture which simulates the actual operating conditions. The fuel piston assembly (8002719) will be assembled in the fuel side of the start valve per drawing 2-066739 for the burst test on the fuel diaphragm (1103290-3). For the oxidizer diaphragm (1103290-1) the oxidizer piston assembly (8002213) will be assembled in the oxidizer side of the valve per 2-066739. The helium diaphragm (2-063994-3) will be tested in the relief elbow assembly (2-063994-3). The propellant diaphragms (2045074) for the Aerobee 150 will burst in the case assembly (2-016589) using a 2-01659-2 retainer.

Where applicable, bolts securing the diaphragm to the piston assembly will be torqued to 45 in-lbs. Bolts holding the fixture flange cover should be torqued to 70 in-lbs. The rate of nitrogen pressure rise will be regulated to simulate the actual system pressure rise rate.

Table D2

Sample Sizes for Propellant Diaphragm Burst Tests.

Lot Size	Minimum Sample Size
11–110	10
111–180	15
181–300	20

Calculation

On the basis of the burst tests the following statistics are calculated: average burst pressure,

$$\bar{x} = \left[\sum_{i=1}^{n} x_i \right] \frac{1}{n} , \qquad (D1)$$

standard deviation,

$$s = \left[\sum_{i=1}^{n} \frac{x_i^2 - n\bar{x}^2}{n-1} \right]^{1/2} , \qquad (D2)$$

where x_i is the burst pressure of the *ith* sample disc and n = sample size.

Using $\bar{x}$ and s, the upper and lower quality indices, Q_U and Q_L are computed by the following equations:

$$Q_U = \frac{U - \bar{x}}{s}$$

$$Q_L = \frac{\bar{x} - L}{s} , \qquad (D3)$$

where U is the upper acceptance tolerance limit and L is the lower tolerance limit. The acceptable quality limits Q_U and Q_L are shown in Figures D1, D2, and D3. The two limits are given for each diaphragm in Table D3.

Acceptance/Rejection Criteria

If both the calculated value of Q_U and Q_L fall on or above the line corresponding to the appropriate sample size the lot is accepted. If *either* of the values of Q_L or Q_U falls below the appropriate line the lot is rejected.

Table D3

Upper and Lower Acceptance Limits.
(bursting pressure in psi)

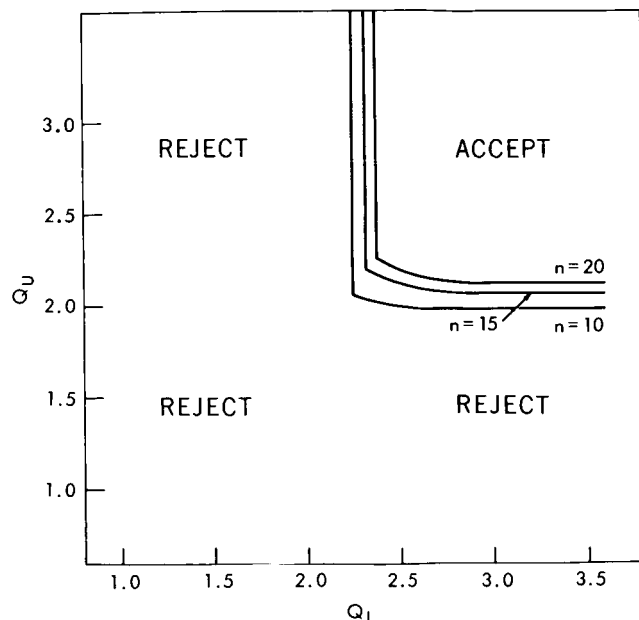| Diaphragm	Upper Limit	Lower Limit
Fuel	375	275
Oxidizer	250	150
Helium	375	125
Propellant	75	25

Figure D2—Aerobee 150A oxidizer diaphram acceptance criteria.
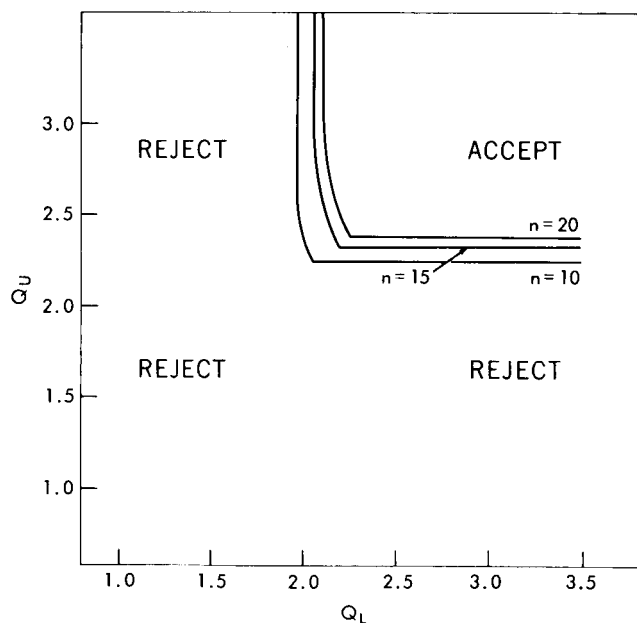

Figure D1—Aerobee 150A fuel diaphram acceptance criteria.
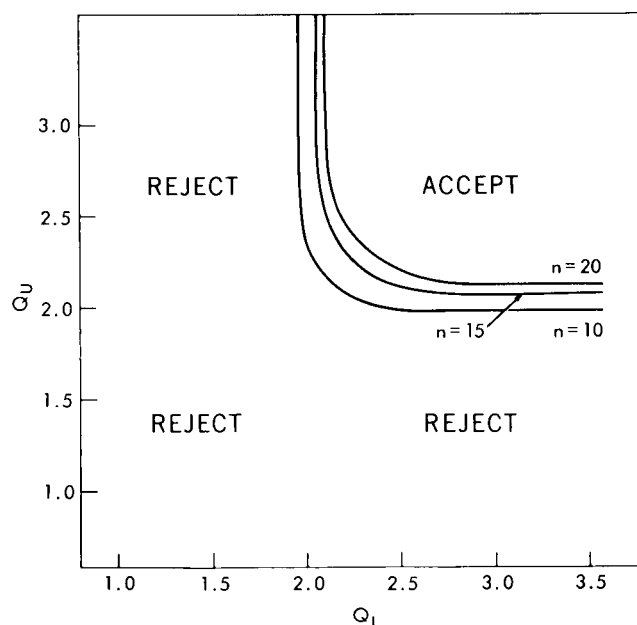

Figure D3—Helium and Aerobee 150A propellant diaphram acceptance criteria.

ARGMA Acceptance Criteria

After a sufficient number of lots have been tested, the required sample size can be reduced by converting the acceptance program from MIL-STD-414 (unknown variance) to the ARGMA

acceptance criteria.* Depending on lot-to-lot variation, 10-20 lots should be inspected before making the conversion. At this point the sample size can be reduced from 10 under the MIL-STD-414 approach to 5 under the ARGMA acceptance plan. In addition to a reduced sample size the ARGMA approach increases control over the quality of incoming diaphragms.

Calculations

Estimate of Population Standard Deviation

After it has been shown that there is no significant lot-to-lot variation, the estimate of the population standard deviation is computed as follows:

$$\hat{\sigma} = \left[\frac{n_1 s_1^2 + n_2 s_2^2 + \cdots n_k^2 s_k^2}{n_1 + n_2 + \cdots n_k - k} \right]^{1/2} , \tag{D4}$$

where n is the sample size of the *ith* lot tested and s_i is the standard deviation of the *ith* lot.

Tolerance Limits

A sample of five discs is drawn at random from each lot regardless of the size of the lot. The mean of each sample is then calculated using Equation D1. The upper and lower tolerance limits are computed as follows:

$$T_L = \bar{x} - k_2 \hat{\sigma} \tag{D5}$$

$$T_U = \bar{x} + k_1 \hat{\sigma}$$

as defined by Equation D4 with k_1 and k_2 given in Table D4 for each diaphragm.

Table D4

Tolerance Limit Constants for Equation D5.

Diaphragm	Constant for Upper Tolerance Limit, k_1	Constant for Lower Tolerance Limit, k_2
Fuel	3.42	3.68
Oxidizer	3.68	3.42
Helium	3.42	3.42
Propellant	3.42	3.42

Acceptance/Rejection Calculated Criteria

If the calculated value of T_U is *less* then the u limit given for each diaphragm in Table D3 the lot is accepted, *if* the calculated value of T_L is *greater* than the L limit given in Table D3. If either of these two criteria is not satisfied the lot is rejected.

---

*"Reliability of Compliance with One-sided Specification Limits when Data is Normally Distributed," ARGMA (Army Rocket and Guided Missile Agency) TR-SBIR, 15 September 1961.

> *"The aeronautical and space activities of the United States shall be conducted so as to contribute . . . to the expansion of human knowledge of phenomena in the atmosphere and space. The Administration shall provide for the widest practicable and appropriate dissemination of information concerning its activities and the results thereof."*

—NATIONAL AERONAUTICS AND SPACE ACT OF 1958

NASA SCIENTIFIC AND TECHNICAL PUBLICATIONS

TECHNICAL REPORTS: Scientific and technical information considered important, complete, and a lasting contribution to existing knowledge.

TECHNICAL NOTES: Information less broad in scope but nevertheless of importance as a contribution to existing knowledge.

TECHNICAL MEMORANDUMS: Information receiving limited distribution because of preliminary data, security classification, or other reasons.

CONTRACTOR REPORTS: Technical information generated in connection with a NASA contract or grant and released under NASA auspices.

TECHNICAL TRANSLATIONS: Information published in a foreign language considered to merit NASA distribution in English.

TECHNICAL REPRINTS: Information derived from NASA activities and initially published in the form of journal articles.

SPECIAL PUBLICATIONS: Information derived from or of value to NASA activities but not necessarily reporting the results of individual NASA-programmed scientific efforts. Publications include conference proceedings, monographs, data compilations, handbooks, sourcebooks, and special bibliographies.

Details on the availability of these publications may be obtained from:

SCIENTIFIC AND TECHNICAL INFORMATION DIVISION

NATIONAL AERONAUTICS AND SPACE ADMINISTRATION

Washington, D.C. 20546